ENVIRONMENTAL RESEARCH
LETTERS

LETTER • **OPEN ACCESS**

Siberian taiga and tundra fire regimes from 2001–2020

To cite this article: Anna C Talucci *et al* 2022 *Environ. Res. Lett.* **17** 025001

IOP Publishing Environ. Res. Lett. 17 (2022) 025001 https://doi.org/10.1088/1748-9326/ac3f07

ENVIRONMENTAL RESEARCH
LETTERS

OPEN ACCESS

RECEIVED
27 July 2021

REVISED
28 November 2021

ACCEPTED FOR PUBLICATION
1 December 2021

PUBLISHED
18 January 2022

LETTER

Siberian taiga and tundra fire regimes from 2001–2020

Anna C Talucci[1], Michael M Loranty[1] and Heather D Alexander[2]

[1] Department of Geography, Colgate University, Hamilton, NY, 13346, United States of America
[2] School of Forestry and Wildlife Sciences, Auburn University, Auburn, AL, 36849, United States of America

E-mail: actalucci@gmail.com

Keywords: wildfire, Siberia, taiga, tundra, fire regimes, climate warming, Landsat

Supplementary material for this article is available online

Abstract

Circum-boreal and -tundra systems are crucial carbon pools that are experiencing amplified warming and are at risk of increasing wildfire activity. Changes in wildfire activity have broad implications for vegetation dynamics, underlying permafrost soils, and ultimately, carbon cycling. However, understanding wildfire effects on biophysical processes across eastern Siberian taiga and tundra remains challenging because of the lack of an easily accessible annual fire perimeter database and underestimation of area burned by MODIS satellite imagery. To better understand wildfire dynamics over the last 20 years in this region, we mapped area burned, generated a fire perimeter database, and characterized fire regimes across eight ecozones spanning 7.8 million km^2 of eastern Siberian taiga and tundra from ∼61–72.5° N and 100° E–176° W using long-term satellite data from Landsat, processed via Google Earth Engine. We generated composite images for the annual growing season (May–September), which allowed mitigation of missing data from snow-cover, cloud-cover, and the Landsat 7 scan line error. We used annual composites to calculate the difference Normalized Burn Ratio (dNBR) for each year. The annual dNBR images were converted to binary burned or unburned imagery that was used to vectorize fire perimeters. We mapped 22 091 fires burning 152 million hectares (Mha) over 20 years. Although 2003 was the largest fire year on record, 2020 was an exceptional fire year for four of the northeastern ecozones resulting in substantial increases in fire activity above the Arctic Circle. Increases in fire extent, severity, and frequency with continued climate warming will impact vegetation and permafrost dynamics with increased likelihood of irreversible permafrost thaw that leads to increased carbon release and/or conversion of forest to shrublands.

1. Introduction

Current-day circum-boreal and -tundra biomes serve as vital carbon sinks that are increasingly vulnerable to climate warming and associated increases in wildfire activity (Gillett 2004, Kasischke and Turetsky 2006, Flannigan *et al* 2009, Mack *et al* 2011, McLauchlan *et al* 2020). Fire directly influences carbon cycling through the combustion of organic material (Kasischke *et al* 2005) and indirectly by altering surface properties such as vegetation cover and composition (Baltzer *et al* 2021, Mack *et al* 2021) that influence subsequent permafrost degradation (Gillett 2004, Flannigan *et al* 2009, Mack *et al* 2011, Abbott *et al* 2016, Holloway *et al* 2020). Understanding the distribution of wildfire activity across northern ecosystems is crucial to identifying feedbacks between vegetation, carbon, albedo, and permafrost that influence climate (Berner *et al* 2012, Loranty *et al* 2016, Chen and Loboda 2018, Holloway *et al* 2020). While North American has an extensive record of wildfire activity (Stocks *et al* 2002, Kasischke and Turetsky 2006), records from eastern Siberia (and Russia in general) are challenging to acquire from internal agencies or limited to moderate to coarse resolution satellite data products that often underestimate burned area (Shvidenko *et al* 2011, Berner *et al* 2012). A more detailed record of fire activity across eastern Siberian taiga (synonymous with boreal) and tundra ecozones is necessary to better

understand spatiotemporal characteristics of fire regimes.

Across Siberian taiga and tundra, fire activity is intricately linked with permafrost degradation through the combustion of vegetation and soils that warm permafrost and increases microbial respiration that releases carbon stores into the atmosphere (Mack *et al* 2011, Loranty *et al* 2016, Alexander *et al* 2018, Holloway *et al* 2020). Much of the region is underlain by continuous permafrost with regions above the Arctic Circle containing Yedoma—thick, carbon- and ice-rich permafrost deposits (Grosse *et al* 2013, Strauss *et al* 2017). The interactive mechanisms of fire and permafrost also influence post-fire vegetation recovery, particularly for larch (*Larix* spp.) forests that cover much of Siberia and grow atop continuous permafrost (Sofronov and Volokitina 2010, Alexander *et al* 2018). Understanding the impacts of changing fire regimes on permafrost stability and related climate feedbacks requires an improved understanding of Siberia taiga and tundra fire regimes.

The current understanding of Siberian fire regimes is spatially and temporally limited, with existing research predominantly focused on western and central regions and little knowledge of fire activity across eastern Siberian taiga and tundra. Annual fire activity has limited ground-based records that are challenging to access and underestimate area burned since all fires are not mapped, compared to coarse spatial resolution satellite-based studies (Soja *et al* 2007). However, coarse spatial resolution satellites miscalculate large fires (Advanced Very High Resolution Radiometer, AVHRR, 1.1 km) (Shvidenko *et al* 2011) and underestimate annual area burned by 40%–50% compared to the finer scale resolution of Landsat (30 m) (Berner *et al* 2012). These underestimations make it challenging to fully understand wildfire dynamics and the changes that are occurring throughout the region. Extreme fire seasons result in increased carbon emissions from soil organic matter combustion (Soja 2004), and there is a rising trend in extreme fire seasons (Soja *et al* 2007, Kirillina *et al* 2020). Extreme fire seasons may also influence vegetation shifts from forest to shrubland or treeline advance (Frost and Epstein 2014, Sizov *et al* 2021) and/or cause irreversible permafrost degradation that does not support larch recruitment (Frost and Epstein 2014). Across northwestern and central Siberia, a rise in fire activity has been attributed to warmer and drier conditions (Soja *et al* 2007, Ponomarev *et al* 2016, Masrur *et al* 2018, Kirillina *et al* 2020) as well as human activity (Kirillina *et al* 2020, Sizov *et al* 2021).

Eastern Siberian taiga and tundra ecosystems are shaped by wildfire activity that contributes to ecological processes and climate feedbacks, but fire dynamics are not well understood. Unprecedented fire seasons over the past several years (Natali *et al* 2021) highlight the need for a fire perimeter database capable of contextualizing fire regime changes by serving as a baseline for long-term monitoring and characterizing the influence of climate change on fire activity. While there are limitations due to missing data before 1996 from the blackout period (Berner *et al* 2012), snow, and clouds, Landsat offers an ecologically meaningful resolution (30 m) that can be readily linked with field data and corresponds with North American fire perimeter and burn severity databases (MTBS 2016). We have three main objectives to understand fire activity across the eight ecozones in the eastern Siberian taiga and tundra. First, we develop a fire perimeter database with the Landsat Archive. Second, we characterize the spatiotemporal components of fire regimes, including annual area burned, fire frequency, fire rotation, fire size classes, and fire season length for each ecozone. Finally, we use statistical models to identify the relationship between annual area burned and key climate drivers—mean summer climate water deficit (hereafter water deficit), mean summer precipitation, mean summer temperature, fire season length, and snowmelt timing.

2. Materials and methods

2.1. Study area

This study focuses on eight ecozones across eastern Siberian taiga and tundra regions where fire is a key ecological disturbance on landscapes that are underlain by continuous permafrost (figure 1). The eight ecozones include Bering tundra, Cherskii-Kolyma Mountain tundra, Chukchi Peninsula tundra, East Siberian taiga, Northeast Siberian coastal tundra, Northeast Siberian taiga, Taimyr-Central Siberian tundra, Trans-Baikal Bald Mountain tundra and span 7.8 million km^2 from ∼61–72.5° N and 100° E–176° W. Each ecozone delineates an area containing similar flora and fauna related to biogeographic realms (Olson *et al* 2001), and ecozone boundaries were publicly available and free (www.worldwildlife.org/publications/terrestrial-ecoregions-of-the-world).

East Siberian taiga and Northeast Siberian taiga are composed predominantly of larch, a deciduous needle-leaf conifer that requires periodic fire to persist on the landscape (Kharuk *et al* 2011). Fire typically spreads across the surface resulting in tree mortality primarily from root damage and consumption of shrubs and the soil organic layer, exposing mineral soils and removing competition, thereby facilitating larch seedling establishment (Sofronov and Volokitina 2010, Alexander *et al* 2018, Kharuk *et al* 2021). The southwestern portion of the study area gives way to forests of Scots pine (*Pinus sylvestris*), a fire-adapted species that require periodic fires that burn as surface and crown fires resulting in tree mortality

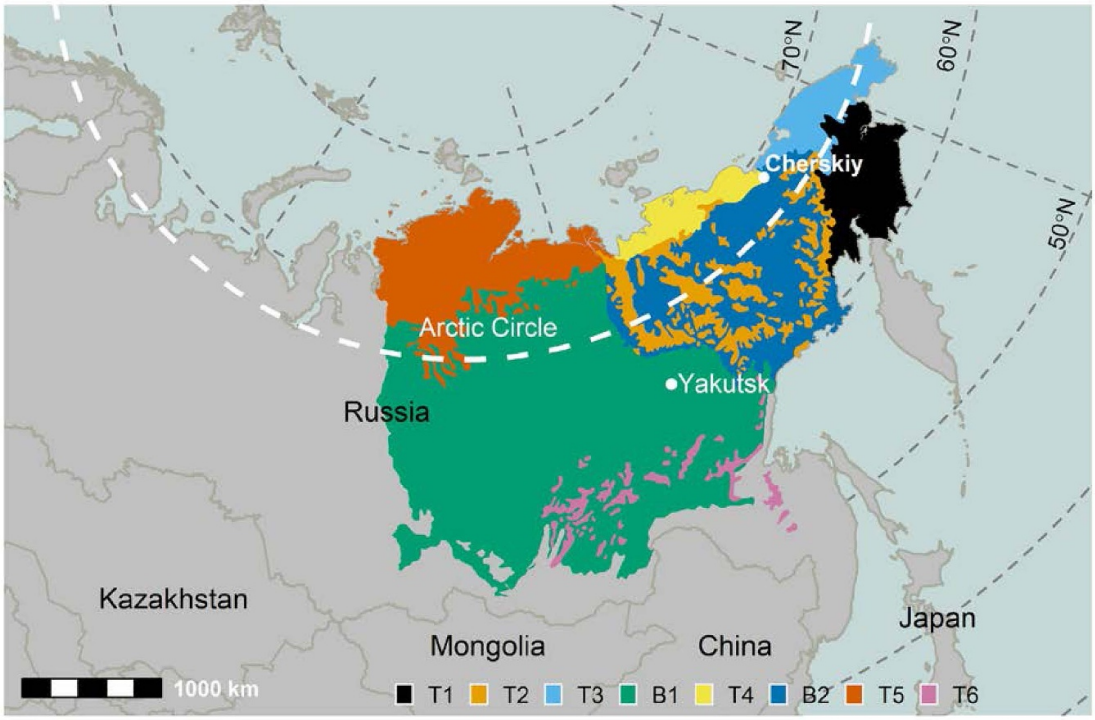

Figure 1. The study area spanned eight ecozones across the boreal forest and tundra biomes of Eastern Siberia: East Siberian taiga (B1), Northeast Siberian taiga (B2), Bering tundra (T1), Cherskii-Kolyma Mountain tundra, (T2), Chukchi Peninsula tundra (T3), Northeast Siberian coastal tundra (T4), Taimyr-Central Siberian tundra (T5), and Trans-Baikal Bald Mountain tundra (T6). The ecozone shapefile was developed by Olson *et al* (2001) and is freely available through the World Wildlife Fund (www.worldwildlife.org/publications/terrestrial-ecoregions-of-the-world). The white dashed line indicates the Arctic Circle. Also shown are the city of Yakutsk and the urban locality of Cherskiy.

(Kharuk *et al* 2011, 2021). Northern latitudes transition to forest-tundra and then tundra zones composed of graminoids, prostrate shrubs, erect shrubs, and wetlands (Walker *et al* 2010).

2.2. Fire perimeter product

We generated an annual fire perimeter database from 2001 to 2020 using the Landsat archive (30 m resolution) (Wulder *et al* 2016) for the study area using Google Earth Engine (hereafter Earth Engine) (Gorelick *et al* 2017) and the R Statistical Computing Software (R Core Team 2018). The time frame was selected due to the overlap with MODIS Collection 6 (i.e. hotspots) that detect thermal anomalies and the best available Landsat imagery due to a lack of imagery prior to 1996 from the blackout period (Berner *et al* 2012). Landsat was chosen because of the spatial-temporal coverage, specifically, the finer spatial resolution (30 m) compared to MODIS (500 m) that would align with burn severity mapping in North America (Key and Benson 2006, Eidenshink *et al* 2007, Wulder *et al* 2016) that relies on the long temporal record 1984–present. The spatial scale of Landsat would allow for future research addressing pertinent ecological questions about post-fire landscapes that depend on ecologically meaningful scales. The 30 m resolution of Landsat maintains finer-scale features that are lost at coarser resolutions like MODIS (Turner *et al* 1989, Benson and MacKenzie 1995). The methods to delineate fire perimeters around burned areas were assessed with an existing fire perimeter dataset from the 2004 Alaskan fire season (see supplementary material (available online at stacks.iop.org/ERL/17/025001/mmedia)). Due to computational limits in Earth Engine, the study area was split into three regions of interest (ROIs) to process imagery and apply the vectorization function for each fire season.

We used the Landsat 5, 7, and 8 Surface Reflectance Tier 1 products that were harmonized for corresponding bands (Roy *et al* 2016). We selected growing season months (May–October), masked pixels covered by snow and clouds, and then generated annual composite images using the best pixel approach (Hermosilla *et al* 2015). Composite images allowed us to mitigate missing data from snow-cover, cloud-cover, and the Landsat 7 scan line error. We used one-year prefire and one-year post-fire annual composites to calculate the difference Normalized Burn Ratio (dNBR) (Eidenshink *et al* 2007) for each fire year using the extended assessment outlined by Key and Benson (2006). Each annual dNBR image was converted to a binary burned/unburned image.

Delineating fire perimeters relied on the binary image. We created polygons from MODIS hotspot data to constrain the extent of computational

processing. We buffered the hotspot point data by 3 km and converted them into polygons with the 'sf' (Pebesma 2018) package in R. The purpose of transforming points to polygons and buffing by 3 km was to limit the spatial extent of the vector algorithm so we would remain within computational limits of Earth Engine. We visually compared the 3 km with both smaller and larger buffers. However, the 3 km buffers allowed us to stay within the computational limits and capture the extent of the wildfire. The fire perimeters were delineated around Landsat pixels with the vectorize function in Earth Engine and exported as shapefiles. The shapefiles were cleaned in R with the 'sf' (Pebesma 2018) and 'spatialeco' (Evans 2021) packages. The three ROIs were combined, and polygons were buffered at 1000 m to combine any adjacent polygons. We then removed any holes within the polygons and converted them from multi-polygon to individual polygons. We applied a −1000 m buffer once holes were removed to counteract the first 1000 m buffer. Finally, we used a smoothing and simplification function with the 'smoothr'(Strimas-Mackey 2021) and 'rmapshaper' (Teucher *et al* 2021) package respectively, to reduce the pixelated appearance and number of vertices.

We created attributes to characterize each fire perimeter with the 'tidyverse' package (Wickham *et al* 2019). We assigned each fire perimeter its majority ecozone, a location of either arctic or subarctic, and a permafrost designation of continuous or discontinuous. We summarized the MODIS hotspot data to assign a start and end day and confidence levels as mean, maximum, and minimum to each fire perimeter. We calculated the area for each fire perimeter in hectares (ha) and assigned a unique fire ID. We assigned a fire size class based on the perimeter area following the Canadian large fire database (Stocks *et al* 2002). While there is not globally common language to characterize fire size (Burton *et al* 2008, Stephens *et al* 2014, Tedim *et al* 2018), we describe small fires as <1000 ha, moderate fires as 1000 < 10 000 ha, large fires as 10 000 < 50 000 ha, extremely large fires as 50 000 < 100 000 ha, and mega-fires as ≥ 100 000. We removed any fire perimeters with zero percent confidence per the MODIS hotspot data measures. We chose to retain other low confidence intervals because fires burn less intensely in the Russian taiga compared to the North American boreal (Wooster 2004), needle-leaf forests tend to see lower confidence levels than open landscapes (Roy *et al* 2008), and cloud cover is a persistent issue (Warren *et al* 1986). Many of the fires with lower confidence were smaller. Fire perimeters less than 200 ha were removed to match similar database criteria in North America (Stocks *et al* 2002). The fire perimeter database is available through the Arctic Data Center (Talucci *et al* 2021).

To assess the fire perimeter product, we visually compared the vectors generated in Earth Engine with fire perimeters from the 2004 Alaska fire season. Alaska fire perimeters were downloaded from Monitoring Trends in Burn Severity (MTBS 2016). The MTBS perimeters are generated with various techniques, including aerial surveys, image digitization, and combinations thereof. We implemented the process described above and then visually inspected the alignment and coverage of our vectors with MTBS vectors (MTBS 2016). Additionally, we compared the Landsat scale fire perimeter database to the MODIS burned area product to quantitatively assess differences.

2.3. Analysis of fire regimes and climate controls

To provide a foundational understanding of fire activity from 2001 to 2020, we characterized spatiotemporal attributes of fire regimes across ecozones. We summarized each ecozone's annual area burned, number of fires per year, area burned by fire size class, fire season length and timing, and fire rotation. Fire rotation refers to the time it takes to burn the area equivalent to the landscape and is calculated as the time of study period divided by the proportion of area burned (Heinselman 1973, Bond and Keeley 2005, Berner *et al* 2012). For example, in the Northeast Siberian Taiga zone, we divide the 20 year study period by the total proportion of area burned within the ecozone that burned during the study period, 0.159 (i.e. total area burned, 19 295 km^2, divided by the area of the ecozone 1133 262 km^2) resulting in a fire rotation of 126 years.

We examined trends in annual area burned as they related to climate factors—mean summer water deficit, mean summer precipitation, mean summer maximum temperature, fire season length, and snowmelt timing—with linear models. There are few evaluations of climate and fire in Siberian taiga and tundra (Balzter *et al* 2005). Precipitation (Balzter *et al* 2005), temperature (Balzter *et al* 2005), and water deficit (Stephenson 1998, Abatzoglou and Williams 2016, Abatzoglou *et al* 2018) are important drivers of fire activity (Gillett 2004, Flannigan *et al* 2009). In Earth Engine, we extracted monthly means for water deficit, precipitation, and temperature by year for each fire perimeter and ecozone from the TerraClimate dataset (Abatzoglou *et al* 2018). In R, climate values were calculated for each year as the mean summer maximum temperature and mean summer precipitation from April to September following Balzter *et al* (2005), mean accumulated water deficit from April to September for perimeters within each ecozone. Annual ecozone values were calculated similarly and used for ecozones and years with zero annual area burned. We calculated the first day of snowmelt with MODIS Terra snow cover daily global 500 m

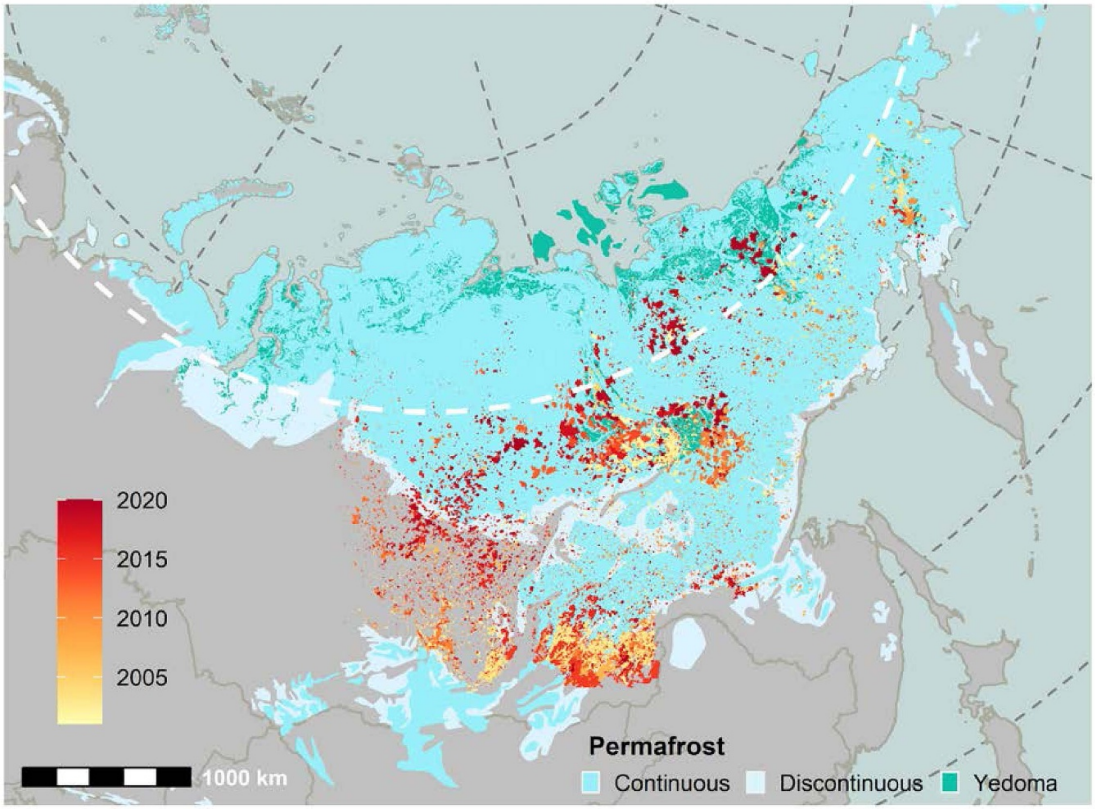

Figure 2. Across eastern Siberian taiga and tundra, the area burned between 2001 and 2020. Continuous and discontinuous permafrost areas are shown as well as the thick, ice-rich Yedoma. The Arctic Circle is delineated by the white dashed line.

product (MOD10A1 V6) in Earth Engine. Snowmelt was extracted as a mean for each fire perimeter and each ecozone in Earth Engine. In R, an annual mean snowmelt date was calculated for each ecozone based on fire perimeter values, and for years with zero annual area burned, snowmelt days came from ecozone values. Fire season length was calculated from the minimum start day and maximum end day for fire perimeters within the ecozone.

3. Results

3.1. Fire perimeter product

We mapped 22 110 fires burning 150.5 million hectares (Mha) over 20 years (figure 2). We found that vectors from Earth Engine align well with MTBS vectors (figure A1). Where multiple large fire events merged and were delineated with separate perimeters in MTBS, our approach resulted in a single polygon. The estimated area differences between the fire perimeter product and MTBS compared favorably both over and underestimating (figure A1). The MODIS burned area product often underestimated area burned compared to the estimates from the fire perimeter database. Over the 20 year timeframe, MODIS underestimated the area burned by ∼48% (−4.9%–78.6%; table 1).

3.2. Fire regimes

Across ecozones, fire activity showed interannual spatiotemporal variability in area burned and the number of fires (figures 2–4). Annual area burned and the number of fires per year exhibited similar patterns for each ecozone, with larger area burned corresponding to more fire events and smaller annual area burned corresponding to fewer fire events (figures 3(a) and (b)). The taiga zones (East Siberian and Northeast Siberian Taiga) were large contributors to annual area burned (figures 3(a), (b), (e) and (f)), with tundra regions accounting for a much smaller portion of annual area burned corresponding with lower fire frequency. The largest fire year based on the total annual area burned for all ecozones was 2003, with East Siberian taiga and Bering tundra being large contributors to the total (table 2). The 2020 season was the largest fire year for Northeast Siberian Taiga, Cherskii-Kolyma mountain tundra, Northeast Siberian coastal tundra, and Chukchi Peninsula tundra, with many large fires burning above the Arctic Circle (figure 2 and table 2). The average annual area burned was highest in the East Siberian taiga, ∼6 Mha, followed by Northeast Siberian Taiga with ∼0.9 Mha (table 3), with the Bering tundra, Cherskii-Kolyma mountain tundra, Chukchi Peninsula tundra, Northeast Siberian coastal tundra, Taimyr-Central

Table 1. Comparison between annual area burned of fire perimeter product and MODIS area burned product. We report the annual area burned for Landsat and MODIS, the difference between Landsat and MODIS, the percent difference, and then calculations for the 20 years.

Fire year	Landsat total annual area burned (ha)	MODIS total annual area burned (ha)	Difference in annual area burned (ha; Landsat-MODIS)	Percent difference (%)
2001	5032 601	3109 675	1922 926	38.2
2002	14 455 758	5327 506	9128 252	63.1
2003	22 207 480	8961 313	13 246 167	59.6
2004	813 824	920 693	−106 869	−13.1
2005	2161 571	1784 351	377 220	17.5
2006	3789 094	2405 165	1383 929	36.5
2007	5582 193	1196 336	4385 857	78.6
2008	3990 463	4185 565	−195 102	−4.9
2009	2912 290	2156 204	756 086	26.0
2010	3690 995	2694 739	996 256	27.0
2011	9227 404	4337 350	4890 054	53.0
2012	7744 747	5054 783	2689 964	34.7
2013	4800 784	3126 182	1674 602	34.9
2014	9207 413	5528 963	3678 450	40.0
2015	9111 646	2877 500	6234 146	68.4
2016	9067 524	4452 600	4614 924	50.9
2017	4536 944	3319 332	1217 612	26.8
2018	7178 752	4596 014	2582 738	36.0
2019	11 610 258	6106 760	5503 498	47.4
2020	13 383 348	6288 662	7094 686	53.0
Total	150 505 089	78 429 693	72 075 396	47.9

Siberian tundra, Trans-Baikal Bald Mountain tundra averaging a smaller annual area burned (table 3). We standardized the mean number of fires per 10 000 km^2, which averaged 2.1 for East Siberian taiga and 1.2 For Northeast Siberian Taiga. At the same time, tundra zones saw a decrease in the mean number of fires per 10 000 km^2 along the south to north latitudinal gradient (table 3). Area burned in the Arctic increased substantially in 2019 and 2020, with 3.4 Mha burned in 2019 and 5.4 Mha burned in 2020 representing four- and six-fold increases over the 0.9 Mha burned in the previous largest year (2018) (figure 4 and table A2). For the 20 years, the fire rotation varied by ecozone, with East Siberian taiga having the shortest rotation at 65 years, followed by Northeast Siberian Taiga at 126 years. The tundra zones showed fire rotation increases from south to north (table 3).

Across ecozones, the distribution of fire size classes varied with annual area burned and the number of fires (figure 5). For East Siberian taiga and Northeast Siberian Taiga, large annual area burned was predominantly driven by mega-fire events >100 000 ha, and small fires <1000 ha were more frequent. This pattern occurred for the Bering tundra, Northeast Siberian coastal tundra, and Trans-Baikal Bald Mountain tundra. For Cherskii-Kolyma mountain tundra, Chukchi Peninsula tundra, and Taimyr-Central Siberian tundra ecozones, annual area burned was driven by moderate to large fire events between 2000 < 20 000 ha, and small fires <1000 ha were more frequent.

Fire season length and timing (e.g. start and end) showed interannual variability across ecozones (figure 6 and table 3). The Bering tundra, Cherskii-Kolyma mountain tundra, Chukchi Peninsula tundra, Northeast Siberian coastal tundra, and Taimyr-Central Siberian tundra had the shortest mean fire season length, where some years had zero days of burning. The Trans-Baikal Bald Mountain tundra had the most extended season of the tundra zones. The Northeast Siberian Taiga fire season averaged 138 days while the East Siberian taiga fire season was the longest averaging 224 days.

3.3. Climate factors and annual area burned

Climate factors—water deficit, precipitation, temperature, season length, and snowmelt timing—influenced annual area burned to varying degrees across ecozones (figure 7 and table 4). As water deficit increased, conditions became drier, resulting in an increased annual area burned across all ecozones with variability in model fit (R^2 0.03–0.67). As precipitation decreased, annual area burned increased across all ecozones with variability in model fit (R^2 −0.05–0.48). As the temperature increased, annual area burned increased across all ecozones, with variability in model fit (R^2 0.04–0.87), and Northeast Siberian coastal tundra had a strong model fit. As fire season length increased, annual area burned increased across all ecozones with variability in model fit (R^2 0.15–0.57). Earlier snowmelt corresponded to increased annual area

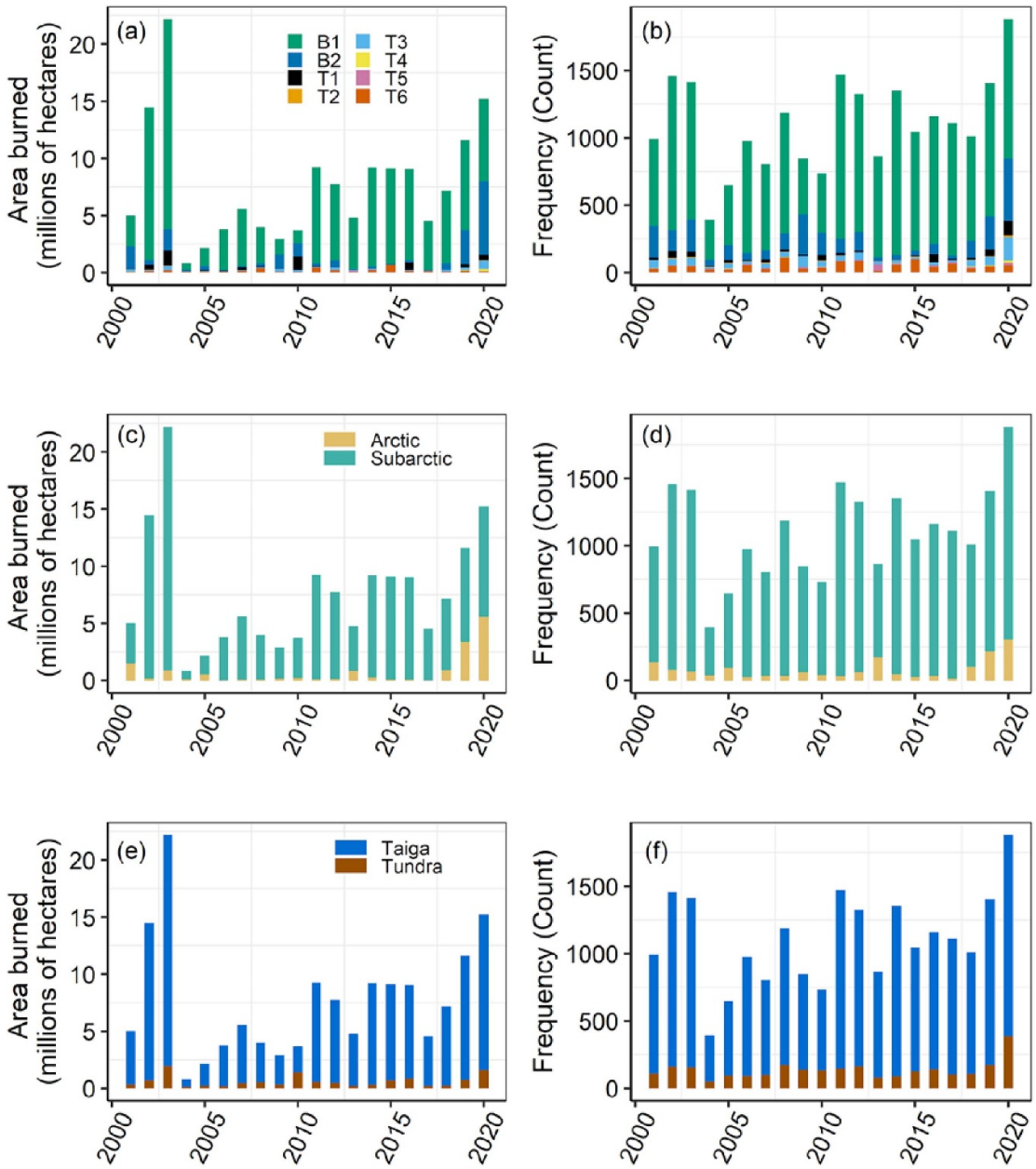

Figure 3. The annual area burned (a) and fire frequency (b) across eight ecozones in eastern Siberian taiga and tundra regions, including East Siberian taiga (B1), Northeast Siberian taiga (B2), Bering tundra (T1), Cherskii-Kolyma Mountain tundra (T2), Chukchi Peninsula tundra (T3), Northeast Siberian coastal tundra (T4), Taimyr-Central Siberian tundra (T5), and Trans-Baikal Bald Mountain tundra (T6). Additional plots show area burned and frequency based on Arctic and Subarctic locations (c), (d) and taiga and tundra biomes (e), (f). See table 2 and A2 for values.

burned for all ecozones with variability in model fit (R^2 0.03–0.67).

4. Discussion

Characterizing fire regimes with satellite-based approaches across eastern Siberian taiga and tundra zones is vital for understanding fire dynamics in areas increasingly vulnerable to climate warming (Gillett 2004, Kasischke and Turetsky 2006, Flannigan *et al* 2009, Mack *et al* 2011, McLauchlan *et al* 2020). We have created a fire perimeter database that improves understanding of fire frequency and distribution across the region over the past 20 years and can support further investigation of heterogeneity in burn severity and subsequent effects on ecosystem function and recovery. Interannual variability in area burned was primarily driven by climatic controls, and large fires dominated years with high annual area burned. Years with large annual area burned typically exhibited regional clustering, with the notable exception of 2020, when fire was extensive across the region, and half of the ecozones experienced their greatest fire seasons in the last 20 years. Our results will serve as a baseline to elucidate long-term shifts in fire regimes.

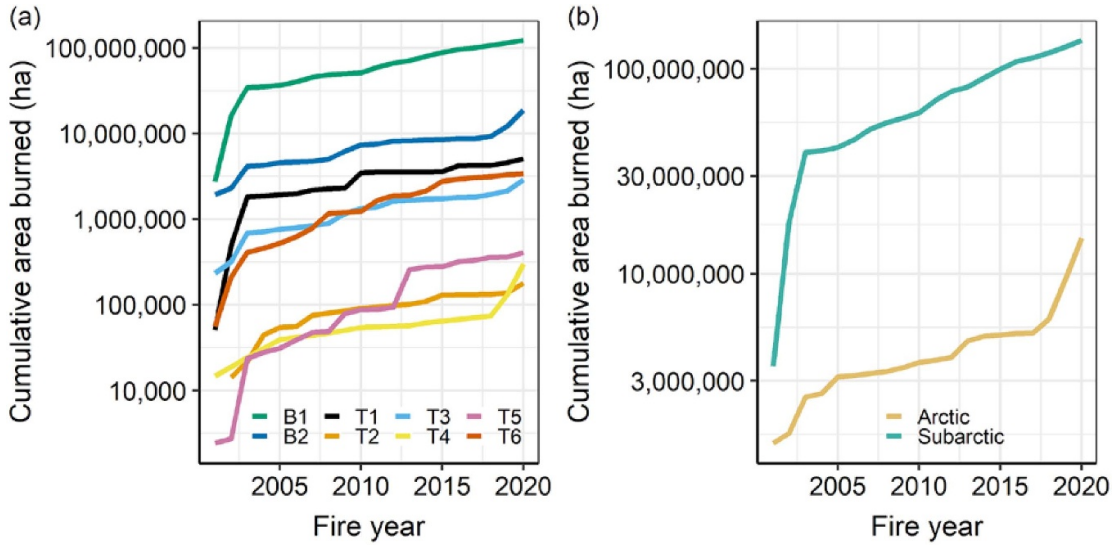

Figure 4. Plots show the cumulative area burned by ecozones (a) and by Arctic or Subarctic location (b). The cumulative area burned varies by ecozone—East Siberian taiga (B1), Northeast Siberian taiga (B2), Bering tundra (T1), Cherskii-Kolyma Mountain tundra (T2), Chukchi Peninsula tundra (T3), Northeast Siberian coastal tundra (T4), Taimyr-Central Siberian tundra (T5), and Trans-Baikal Bald Mountain tundra (T6). The cumulative area burned by the Arctic or subarctic location highlights the substantial uptick in area burned in 2019 and 2020 in the Arctic (b), which corresponds with increases in area burned for Northeast Siberian taiga, Cherskii-Kolyma Mountain tundra, Chukchi Peninsula tundra, and Northeast Siberian coastal tundra in 2019 and 2020. The *y*-axis was log-transformed (base 10) for area burned in hectares (ha). The *x*-axis shows the years 2001–2020.

Table 2. Table of annual area burned for each of eight ecozones. The total annual area burned across the entire region is tallied in the column furthest to the right, while the total area burned between 2001 and 2020 for each ecozone is tallied across the final row. The largest area burned during a fire season for each ecozone is in bold.

	Taiga biome		Tundra biome						
Year	East Siberian taiga (B1)	Northeast Siberian taiga (B2)	Bering tundra (T1)	Cherskii-Kolyma mountain tundra (T2)	Chukchi Peninsula tundra (T3)	Northeast Siberian coastal tundra (T4)	Taimyr-Central Siberian tundra (T5)	Trans-Baikal Bald Mountain tundra (T6)	Total annual area burned (ha)
2001	2742 514	1929 395	50 816	234 819	—	14 743	2419	55 708	5032 414
2002	13 394 713	366 046	440 703	82 527	14 257	—	300	155 222	14 455 768
2003	**18 440 667**	1831 323	**1334 839**	370 739	7337	—	20 691	199 873	22 207 472
2004	567 160	107 733	43 201	20 804	22 960	—	4288	45 672	813 822
2005	1604 952	339 192	60 867	52 592	9872	24 601	3130	64 362	2161 571
2006	3566 438	43 647	43 272	26 532	1117	—	8032	97 859	3788 902
2007	5032 992	99 644	208 753	45 477	19 448	—	8753	165 134	5582 207
2008	3189 529	258 267	87 550	57 052	4679	7531	1325	382 516	3990 456
2009	1313 271	1228 947	26 389	273 523	—	—	29 862	38 284	2912 284
2010	1119 592	1172 038	1165 665	173 767	11 035	7313	8557	31 016	3690 994
2011	8431 207	229 388	71 491	57 856	3709	—	806	430 748	9227 216
2012	6697 355	567 600	17 192	233 542	4018	—	5407	217 635	7744 761
2013	4492 327	81 692	—	34 317	2564	2889	**164 292**	20 694	4800 787
2014	8695 147	180 525	376	60 194	8801	4687	18 912	236 552	9207 208
2015	8339 446	83 192	24 849	13 625	19 645	—	1882	**626 989**	9111 643
2016	8028 168	177 628	622 004	47 839	—	—	39 399	150 470	9067 523
2017	4303 835	33 856	26 926	18 348	—	—	13 110	138 644	4536 737
2018	6391 194	526 533	12 051	142 912	2711	12 147	26 314	62 869	7178 747
2019	7898 818	2977 529	302 771	194 616	5292	56 144	2344	170 720	11 610 252
2020	7250 273	**6413 133**	508 774	**734 728**	**40 398**	**169 967**	45 546	79 829	15 244 668
Total area	121 499 598	18 647 306	5048 487	2875 807	177 843	300 021	405 366	3370 796	152 365 432

Table 3. Fire regime characteristics for 2001–2020. For each of the eight ecozones, we report the mean annual area burned, mean annual fire frequency, the largest fire, the fire rotation, and the mean fire season length, along with the range of variability.

Biome	Taiga		Tundra					
Ecozone	East Siberian taiga (B1)	Northeast Siberian taiga (B2)	Bering tundra (T1)	Cherskii-Kolyma mountain tundra (T2)	Chukchi Peninsula tundra (T3)	Northeast Siberian coastal tundra (T4)	Taimyr-Central Siberian tundra (T5)	Trans-Baikal Bald Mountain tundra (T6)
Mean Annual area burned in ha yr^{-1} (standard error)	6074 980 (977 432)	932 365 (338 877)	265 710 (90 477)	143 790 (38 517)	11 115 (2578)	33 336 (17 931)	20 268 (8149)	168 540 (34 588)
Mean number of fires per year per 10 000 km^2 (range)	2.1 (0.8–3.1)	1.2 (0.2–4.1)	0.6 (0–2.3)	0.8 (0.2–3.1)	0.1 (0–0.4)	0.2 (0–0.7)	0.1 (0–0.5)	2.3 (0.7–5.0)
Largest fire size (ha)	10 866 634	710 545	401 565	119 005	14 758	122 896	27 287	229 300
Fire Rotation (years)	65	122	189	390	3380	1495	4747	130
Mean fire season length in days (range)	224 (193–244)	138 (81–193)	90 (4–164)	91 (19–128)	27 (0–70)	40 (1–68)	111 (0–190)	155 (60–226)

4.1. Fire perimeter database

Satellite imagery is paramount to developing a fire perimeter database and gaining an accurate understanding of fire regimes characteristics, including annual area burned, (Soja 2004) across eastern Siberian taiga and tundra zones. Developing a fire perimeter database is a computationally intensive task made easier by Earth Engine, which allowed us to map fire across eastern Siberia at a spatial resolution comparable to North American fire databases by generating Landsat composite images that mitigated missing data caused by weather and the scanline error from Landsat 7 (Hermosilla *et al* 2015). Fire perimeters developed using our approach matched closely with fire perimeters from Alaska 2004 in the MTBS database, except for large fires in close proximity that merged into a single fire perimeter. Where our approach merged large fires into a single fire complex, MTBS often delineated multiple individual fire events with overlapping boundaries. Previous fire spread research in northern Siberia has noted that large fires in close proximity may merge to form fire complexes (Loboda and Csiszar 2007).

We found that the MODIS product underestimated the area burned by ∼48% over the 20 years. This result aligns with a similar comparison between Landsat and MODIS over a smaller transect in Northeastern Siberia, where MODIS underestimated by ∼40% (Berner *et al* 2012). Several studies utilizing AVHRR (1.1 km) note a miscalculation of large fire events (Soja *et al* 2006, Shvidenko *et al* 2011). Underestimation of the area burned will lead to errors in quantifying regional ecological and climatic consequences of fire. Typically, the spatial extent of large fires is underestimated (Shvidenko *et al* 2011), and these are significant contributors to annual area burned. This miscalculation is likely a function of the pixel resolution (500 m), cloud cover, and detection of false positives (Roy *et al* 2005, 2008). Our fire perimeter product and MTBS varied with both overestimates and underestimates. These differences could depend on when the MTBS perimeter was drawn, with many perimeters hand digitized or drawn with field GPS points. We used composite images, where MTBS uses single scenes, likely contributing to this discrepancy. Cloud cover is a significant issue in Siberia, with summer cloud coverage averaging 60% (Warren *et al* 1986). Our product is based on the difference between imagery from one-year prefire and one-year post. It is not solely reliant on the intensity measures from MODIS, which can be obscured by clouds and smoke. Further, thermal intensities are lower for Siberian Taiga fires, which are predominantly surface fires (Krylov *et al* 2014), compared to the prevalence of crown fires in North American boreal ecosystems (Wooster 2004). Surface fires are more likely to be obscured by surviving live tree canopies and not accounted for in a burned pixel (Kolden *et al* 2012, Krylov *et al* 2014); however, by delineating fire perimeters, using Landsat and MODIS imagery we capture a range of burn severities that likely includes low severity fires where canopy trees survive and unburned refugia (Kolden *et al* 2012) that are commonly missed by MODIS alone. The combination of clouds, lower intensity burning, and overestimates of small and underestimates of large fires all contribute to discrepancies between our estimates from fire perimeters and MODIS burned area product.

4.2. Fire regime characteristics

We quantify baseline fire regime characteristics, including annual area burned and the number of

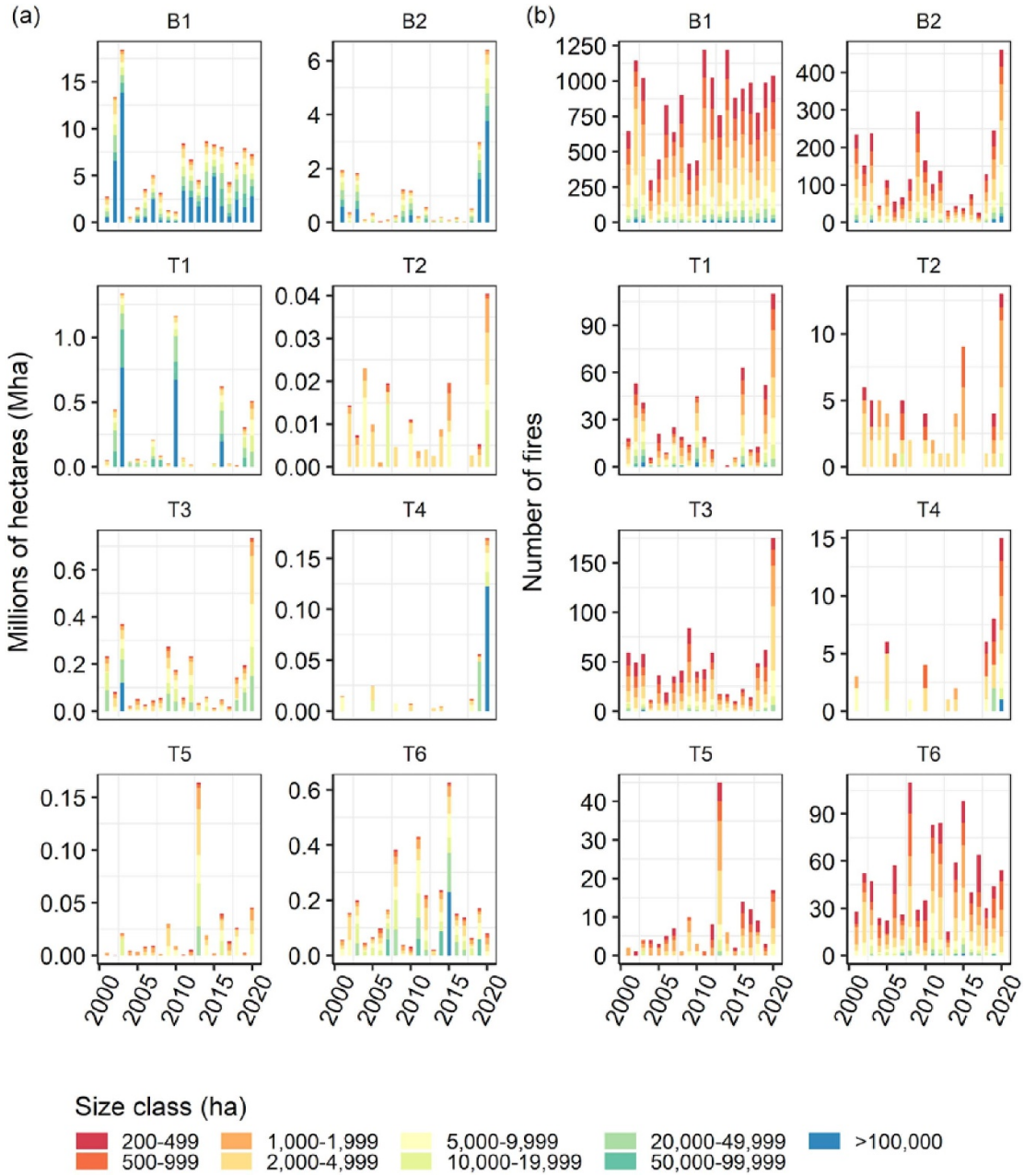

Figure 5. Fire size classes by annual area burned (a) and the number of fires (b) for each of eight ecozones, including East Siberian taiga (B1), Northeast Siberian taiga (B2), Bering tundra (T1), Cherskii-Kolyma Mountain tundra (T2), Chukchi Peninsula tundra (T3), Northeast Siberian coastal tundra (T4), Taimyr-Central Siberian tundra (T5), and Trans-Baikal Bald Mountain tundra (T6). Large fire years are dominated by fires <10 000 ha, while fires >10 000 are more frequent but account for less area burned. For Northeast Siberian coastal tundra (T4), and Northeast Siberian taiga (B2), 2019 and 2020 were exceptionally large fire years for the region with large fire events occurring.

fires across the region, that improve understanding of regional fire dynamics over the last 20 years. The largest fire year across all ecozones was 2003, and this was primarily driven by the area burned in the Eastern Siberia Taiga. Soja *et al* (2006) noted 2003 as a large fire year, although 2003 was not included in their study. Shvidenko *et al* (2011) estimated annual area burned averaged 8 Mha between 1997 and 2010 across Russia, while across our study, the average annual area burned for the last 20 years was 7.5 Mha, indicating that more area is burning across Russia than has been previously estimated. The mean annual area burned across Canada is ∼2 Mha with some years burning ∼7 Mha (Stocks *et al* 2002), and 1–3 Mha burned annually in Alaska (Kasischke and Turetsky 2006). Russian records indicate wildfire seasons are longer and area burned has increased between 1996 and 2018 (Kirillina *et al* 2020). Still, Russian records have been shown to underestimate area burned (Soja *et al* 2006). Few studies cover the eastern portions of Siberia, and differences in spatial extent and temporal coverage between ours and previous studies make direct comparisons difficult (e.g. Soja 2004, Soja *et al* 2006, 2007, Berner *et al* 2012).

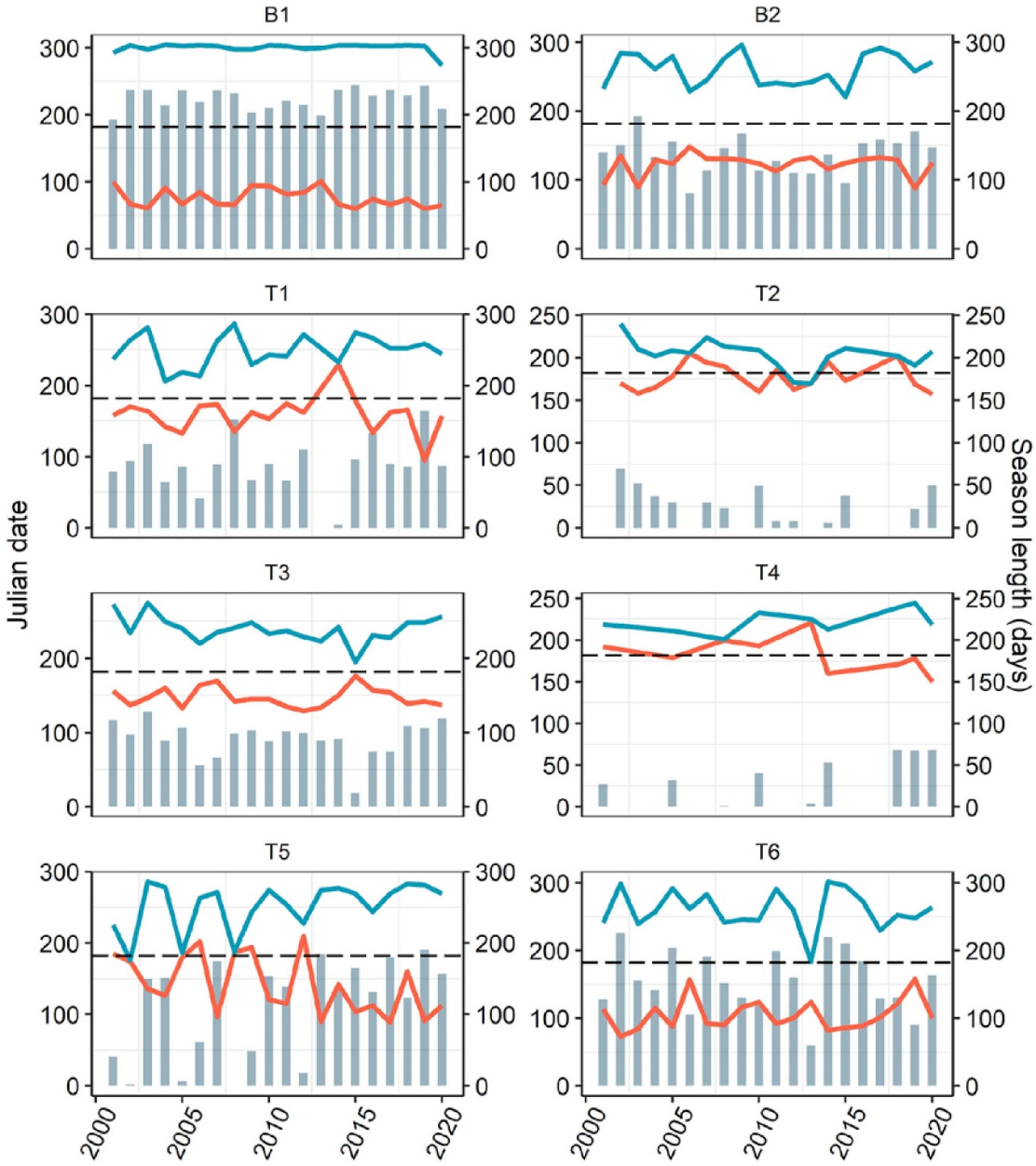

Figure 6. Estimate annual fire season length in each of eight ecozones including East Siberian taiga (B1), Northeast Siberian taiga (B2), Bering tundra (T1), Cherskii-Kolyma Mountain tundra (T2), Chukchi Peninsula tundra (T3), Northeast Siberian coastal tundra (T4), Taimyr-Central Siberian tundra (T5), and Trans-Baikal Bald Mountain tundra (T6). Fire season timing and length vary by ecozone. Note the left *y*-axis is Julian date (lines, red for start day and blue for the end day) and the right *y*-axis is season length (bars). The black dashed line is July 1.

Fire rotation and season length varied across ecozones, with taiga zones having shorter rotations than tundra, and a general increase in fire rotation along the south to north latitudinal gradient, similar to other studies (Furyaev *et al* 2001, Soja 2004, Kharuk *et al* 2011, Berner *et al* 2012). The Northeast Siberian Taiga (126 years), Cherskii-Kolyma mountain tundra (382 years), and Northeast Siberian coastal tundra (1166 years) overlapped with portions of the transect evaluated by Berner *et al* (2012), and they noted fire rotations for lowland forest-tundra at 792 years and southern mountain larch at 110 years between 2000 and 2007. Thus, we are likely capturing some combination of lowland forest-tundra in the Cherskii-Kolyma mountain tundra and Northeast Siberian coastal tundra ecozones, and the southern mountain larch overlaps with the Northeast Siberian Taiga. Similarly, our fire rotation estimates for tundra ecozones span a similar range as those calculated by Rocha *et al* (2012) for Alaskan tundra ecosystems. Additionally, the large fires in 2020 may skew the fire rotation estimates as extreme fire years become increasingly important as the length of the study period decreases. Our findings align with predicted positive associations between fire season length and annual area burned (Stocks *et al* 1998).

In 2020, area burned increased substantially along the Arctic Circle, particularly for Northeast Siberian

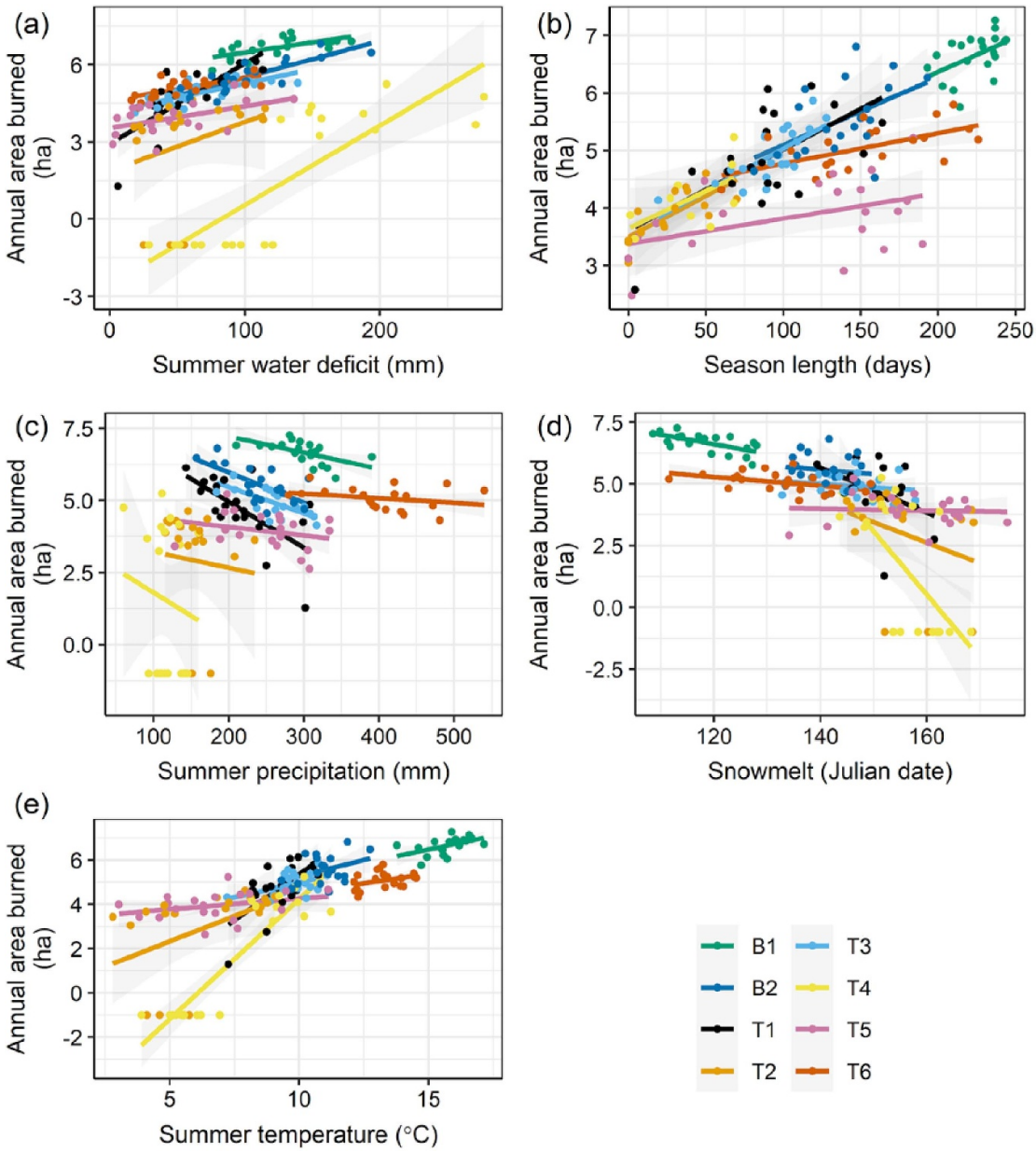

Figure 7. Visualization of linear model trends between annual area burned (*y*-axis) and climate factors—summer water deficit ((a), *x*-axis), fire season length ((b), *x*-axis), summer precipitation ((c), *x*-axis), snowmelt timing ((d), *x*-axis), and summer temperature ((e), *x*-axis), and across eight ecozones—East Siberian taiga (B1), Northeast Siberian taiga (B2), Bering tundra (T1), Cherskii-Kolyma Mountain tundra (T2), Chukchi Peninsula tundra (T3), Northeast Siberian coastal tundra (T4). Taimyr-Central Siberian tundra (T5), and Trans-Baikal Bald Mountain tundra (T6). Model summary statistics are reported in table 4.

Taiga, Cherskii-Kolyma mountain tundra, Northeast Siberian coastal tundra, Chukchi Peninsula tundra, with several large fires occurring above the Arctic Circle. These four ecozones are underlain by continuous permafrost and thick, ice-rich Yedoma permafrost. Over the last 20 years, ∼30% of the total area burned for Northeast Siberian Taiga, Cherskii-Kolyma mountain tundra, and Chukchi Peninsula tundra, and ∼66% of the total area burned for Northeast Siberian coastal tundra occurred in 2020. The increased area burned in the Arctic in 2019 and 2020 may begin to facilitate treeline advance and/or tall shrub expansion (Frost and Epstein 2014, Sizov *et al* 2021). Simultaneously, increased area burn could initiate permafrost degradation limiting larch recruitment and facilitating shrub expansion (Frost and Epstein 2014). Along the taiga-tundra ecotone, where larch forests consist of sparse open-canopy stands, the burn mosaic may enhance larch recruitment in areas of more severe burning, resulting in denser-canopy stands provided there is an available seed source (Alexander *et al* 2018). The increased area burned will influence the heterogeneity of burn mosaics producing multiple post-fire recovery trajectories and changes in permafrost dynamics where waterlogged soils result in recruitment failure

Table 4. Summary of linear models evaluating the trend between annual area burned and summer climate factors—water deficit, precipitation, and temperature, snowmelt, season length—for each of eight ecozones. We report the intercept, slope, R^2, and p-value. Relationships are visualized in figure 7.

Climate factors	Ecozone	Intercept ($ß_0$)	Slope ($ß_1$)	R^2	p-value
Water deficit	East Siberian taiga	5.70	0.01	0.38	0.002
Water deficit	Northeast Siberian taiga	4.09	0.01	0.67	< 0.0001
Water deficit	Bering tundra	2.93	0.03	0.57	< 0.0001
Water deficit	Cherskii-Kolyma Mountain tundra	1.87	0.02	0.03	0.23
Water deficit	Chukchi Peninsula tundra	4.18	0.01	0.56	< 0.0001
Water deficit	Northeast Siberian coastal tundra	−2.54	0.03	0.65	< 0.0001
Water deficit	Taimyr-Central Siberian tundra	3.54	0.01	0.19	0.031
Water deficit	Trans-Baikal Bald Mountain tundra	4.61	0.01	0.39	0.002
Precipitation	East Siberian taiga	8.34	−0.01	0.27	0.01
Precipitation	Northeast Siberian taiga	8.07	−0.01	0.41	0.002
Precipitation	Bering tundra	8.14	−0.02	0.39	0.002
Precipitation	Cherskii-Kolyma Mountain tundra	3.77	−0.01	−0.05	0.74
Precipitation	Chukchi Peninsula tundra	7.30	−0.01	0.48	0.0004
Precipitation	Northeast Siberian coastal tundra	3.42	−0.02	−0.04	0.57
Precipitation	Taimyr-Central Siberian tundra	4.67	0.00	0.01	0.28
Precipitation	Trans-Baikal Bald Mountain tundra	5.72	0.00	0.02	0.25
Temperature	East Siberian taiga	2.81	0.24	0.23	0.02
Temperature	Northeast Siberian taiga	2.27	0.30	0.10	0.1
Temperature	Bering tundra	−2.98	0.83	0.41	0.002
Temperature	Cherskii-Kolyma Mountain tundra	0.04	0.46	0.16	0.05
Temperature	Chukchi Peninsula tundra	2.32	0.27	0.18	0.04
Temperature	Northeast Siberian coastal tundra	−6.59	1.08	0.83	< 0.0001
Temperature	Taimyr-Central Siberian tundra	3.29	0.10	0.04	0.19
Temperature	Trans-Baikal Bald Mountain tundra	2.86	0.17	0.07	0.13
Season length	East Siberian taiga	3.97	0.01	0.19	0.03
Season length	Northeast Siberian taiga	3.92	0.01	0.22	0.02
Season length	Bering tundra	3.61	0.01	0.34	0.005
Season length	Cherskii-Kolyma Mountain tundra	3.50	0.01	0.53	< 0.001
Season length	Chukchi Peninsula tundra	3.56	0.01	0.57	< 0.0001
Season length	Northeast Siberian coastal tundra	3.65	0.01	0.29	0.08
Season length	Taimyr-Central Siberian tundra	3.38	0.00	0.15	0.05
Season length	Trans-Baikal Bald Mountain tundra	4.25	0.01	0.32	0.005
Snowmelt	East Siberian taiga	11.24	−0.04	0.37	0.003
Snowmelt	Northeast Siberian taiga	8.12	−0.02	−0.03	0.55
Snowmelt	Bering tundra	18.33	−0.09	0.15	0.05
Snowmelt	Cherskii-Kolyma Mountain tundra	15.94	−0.08	0.05	0.17
Snowmelt	Chukchi Peninsula tundra	7.01	−0.01	−0.02	0.45
Snowmelt	Northeast Siberian coastal tundra	41.55	−0.26	0.35	0.004
Snowmelt	Taimyr-Central Siberian tundra	4.53	0.00	−0.05	0.79
Snowmelt	Trans-Baikal Bald Mountain tundra	7.38	−0.02	0.14	0.06

(Alexander *et al* 2018). The extent to which changes in fire frequency and distribution will lead to post-fire shifts in vegetation communities remains unclear.

4.3. Climate controls on annual area burned

The annual area burned was influenced by climate factors—water deficit, precipitation, temperature, fire season length, and snowmelt timing—across the region. In taiga zones, annual area burned showed consistent trends with climate factors. In tundra zones, annual area burned was associated with climate factors but the strength of the relationships was variable. Previous work noted that annual area burned has been associated with declines in soil moisture, decreased precipitation, and increased summer temperature (Balzter *et al* 2005, Kharuk *et al* 2011, Masrur *et al* 2018) as well as the Arctic Oscillation (Balzter *et al* 2005). Tundra fire distribution and intensity have been linked to warm, dry conditions that occur from spring into summer (Masrur *et al* 2018). The Arctic Oscillation influences the large-scale weather systems across the region that dictate precipitation, temperature, and soil moisture levels (Balzter *et al* 2005). The water deficit was the most influential variable across the landscape because it provides a better link to ecosystem productivity and moisture levels than temperature or precipitation. It relates to water balance models that combine climatic and biophysical variables (Stephenson 1998, Abatzoglou *et al* 2018). Research shows portions of the region are experiencing longer fire seasons (Kirillina *et al* 2020) that correspond to increases in annual

area burned. Snowmelt likely influences fire activity and area burned, but by itself, it had limited influence. The water deficit captures components of snowmelt timing, precipitation, and temperature that are a more comprehensive measure of interacting climate variables over time (Stephenson 1998, Abatzoglou *et al* 2018). The scale of the climate data is coarse, which is why we looked at annual area burned across ecozones rather than analyzing climatic drivers for individual fires. The fine-scale climate data from local weather stations required for analysis at the individual fire scale are not available. Climate exerts strong control over ecosystem processes at northern latitudes and is considered an important driver to wildfire activity (Flannigan *et al* 2009, Hu *et al* 2015, Young *et al* 2017, Masrur *et al* 2018, Natali *et al* 2021). Climate modeling indicates earlier starts to fire seasons result in climate conditions that contribute to more extreme fire danger across the circumboreal (Stocks *et al* 1998), suggesting that many of these climatic drivers work in concert. Places like Alaska, where regional warming increases fire likelihood in areas such as tundra and treeline that had historically low fire probabilities (Hu *et al* 2015, Young *et al* 2017). Increased fire in these areas would have broader ramifications for ecosystem functions (Rocha *et al* 2012, Alexander *et al* 2018, Holloway *et al* 2020).

5. Conclusion

The Siberian taiga and tundra ecozones are experiencing amplified climate warming more than any other region globally (IPCC 2021). Intensifying fire regimes will impact ecosystems in ways that feedback to global climate (Gillett 2004, Kasischke and Turetsky 2006, Flannigan *et al* 2009, Mack *et al* 2011, Chen and Loboda 2018, McLauchlan *et al* 2020). Our regional fire perimeter database provides comprehensive and foundational knowledge of contemporary fire regime characteristics for this globally important yet relatively understudied region. In addition to refined estimates of annual area burned that capture surface fires often missed by MODIS, our Landsat-derived delineation of individual fire events provide opportunities to examine fine-scale heterogeneity in burn severity and post-fire ecosystem dynamics. The spatial-temporal distribution of fire across eight ecozones demonstrates considerable interannual variability in area burned and the number of fires. Unprecedented high temperatures in 2020 resulted in a six-fold increase in area burned in the Arctic (Natali *et al* 2021). Such extreme fire years are characterized by larger fires, which are otherwise relatively uncommon. Not surprisingly, our analyses indicate that continued warming, drying, and lengthening of the growing season are likely to be accompanied by increases in area burned. Increases in fire extent, severity, and frequency with continued climate warming may foster widespread vegetation change or irreversible permafrost thaw. To quantify regional and global climate feedbacks, it will be crucial to determine whether extreme fire years like 2020 will become more common and to understand the legacy effects of fire on vegetation and permafrost dynamics.

Data availability statement

The data that support the findings of this study are openly available at the following URL/DOI: https://arcticdata.io/catalog/view/doi%3A10.18739%2FA2N87311N.

Acknowledgments

We thank Justin Braaten for helpful conversations regarding Google Earth Engine early on. We thank the developers at Google Earth Engine, as this work would not have been possible without the processing abilities provided by Google Earth Engine. We thank two anonymous reviews whose suggestions clarified and improved this paper. We thank the Colgate University Research Council for funding support. This work was supported by the National Science Foundation, OPP-1708322 to M Loranty and OPP-170837 and OPP-2100773 to H Alexander. Data archiving was provided by the Arctic Data Center.

Author contributions

Conceptualization, M M L, A C T; Data curation A C T; Formal analysis, A C T; Funding Acquisition, M M L, H D A; Investigation, A C T Visualization, A C T; Writing—original draft, A C T, M M L; Writing—review and editing, H D A; All authors have read and agreed to the published version of the manuscript.

Funding

This research was funded by the National Science Foundation, Office of Polar Programs, OPP-1708322 to M. Loranty and OPP-170837 and OPP-2100773 to H. Alexander.

ORCID iDs

Anna C Talucci https://orcid.org/0000-0001-8415-4813
Michael M Loranty https://orcid.org/0000-0001-8851-7386
Heather D Alexander https://orcid.org/0000-0003-1307-8483

References

Abatzoglou J T, Dobrowski S Z, Parks S A and Hegewisch K C 2018 TerraClimate, a high-resolution global dataset of monthly climate and climatic water balance from 1958–2015 *Sci. Data* **5** 170191

Abatzoglou J T and Williams A P 2016 Impact of anthropogenic climate change on wildfire across western US forests *Proc. Natl Acad. Sci. USA* **113** 11770–5

Abbott B W *et al* 2016 Biomass offsets little or none of permafrost carbon release from soils, streams, and wildfire: an expert assessment *Environ. Res. Lett.* **11** 034014

Alexander H D, Natali S M, Loranty M M, Ludwig S M, Spektor V V, Davydov S, Zimov N, Trujillo I and Mack M C 2018 Impacts of increased soil burn severity on larch forest regeneration on permafrost soils of far northeastern Siberia *For. Ecol. Manage.* **417** 144–53

Baltzer J L *et al* 2021 Increasing fire and the decline of fire adapted black spruce in the boreal forest *Proc. Natl Acad. Sci. USA* **118** e2024872118

Balzter H *et al* 2005 Impact of the Arctic Oscillation pattern on interannual forest fire variability in Central Siberia: arctic oscillation pattern *Geophys. Res. Lett.* **32** L14709

Benson B J and MacKenzie M D 1995 Effects of sensor spatial resolution on landscape structure parameters *Landscape Ecol.* **10** 113–20

Berner L T, Beck P S A, Loranty M M, Alexander H D, Mack M C and Goetz S J 2012 Cajander larch (*Larix cajanderi*) biomass distribution, fire regime and post-fire recovery in northeastern Siberia *Biogeosciences* **9** 3943–59

Bond W and Keeley J 2005 Fire as a global 'herbivore': the ecology and evolution of flammable ecosystems *Trends Ecol. Evol.* **20** 387–94

Burton P J, Parisien M-A, Hicke J A, Hall R J and Freeburn J T 2008 Large fires as agents of ecological diversity in the North American boreal forest *Int. J. Wildland Fire* **17** 754

Chen D and Loboda T V 2018 Surface forcing of non-stand-replacing fires in Siberian larch forests *Environ. Res. Lett.* **13** 045008

Eidenshink J, Schwind B, Brewer K, Zhu Z-L, Quayle B and Howard S 2007 A project for monitoring trends in burn severity *Fire Ecol.* **3** 3–21

Evans J S 2021 spatialEco *R Package version* 1.3-6 (available at: https://github.com/jeffreyevans/spatialEco)

Flannigan M, Stocks B, Turetsky M and Wotton M 2009 Impacts of climate change on fire activity and fire management in the circumboreal forest *Glob. Change Biol.* **15** 549–60

Frost G V and Epstein H E 2014 Tall shrub and tree expansion in Siberian tundra ecotones since the 1960s *Glob. Change Biol.* **20** 1264–77

Furyaev V V, Vaganov E A, Tchebakova N M and Valendik E N 2001 Effects of fire and climate on successions and structural changes in the Siberian boreal forest p 16

Gillett N P 2004 Detecting the effect of climate change on Canadian forest fires *Geophys. Res. Lett.* **31** L18211

Gorelick N, Hancher M, Dixon M, Ilyushchenko S, Thau D and Moore R 2017 Google earth engine: planetary-scale geospatial analysis for everyone *Remote Sens. Environ.* **202** 18–27

Grosse G, Robinson J E, Bryant R, Taylor M D, Harper W, DeMasi A, Kyker-Snowman E, Veremeeva A, Schirrmeister L and Harden J 2013 Distribution of late pleistocene ice-rich syngenetic permafrost of the Yedoma Suite in East and central Siberia, Russia (U.S. Geological Survey (available at: https://pubs.usgs.gov/of/2013/1078/)

Heinselman M L 1973 Fire in the virgin forests of the boundary waters Canoe Area, Minnesota *Quat. Res.* **3** 329–82

Hermosilla T, Wulder M A, White J C, Coops N C and Hobart G W 2015 An integrated Landsat time series protocol for change detection and generation of annual gap-free surface reflectance composites *Remote Sens. Environ.* **158** 220–34

Holloway J E, Lewkowicz A G, Douglas T A, Li X, Turetsky M R, Baltzer J L and Jin H 2020 Impact of wildfire on permafrost landscapes: a review of recent advances and future prospects *Permafrost and Periglacial Process* p 2048

Hu F S, Higuera P E, Duffy P, Chipman M L, Rocha A V, Young A M, Kelly R and Dietze M C 2015 Arctic tundra fires: natural variability and responses to climate change *Front. Ecol. Environ.* **13** 369–77

IPCC 2021 *Climate Change 2021: The Physical Science Basis* (Cambridge: Cambridge University Press)

Kasischke E S, Hyer E J, Novelli P C, Bruhwiler L P, French N H F, Sukhinin A I, Hewson J H and Stocks B J 2005 Influences of boreal fire emissions on Northern Hemisphere atmospheric carbon and carbon monoxide: boreal fire emissions *Glob. Biogeochem. Cycles* **19** GB1012

Kasischke E S and Turetsky M R 2006 Recent changes in the fire regime across the North American boreal region—spatial and temporal patterns of burning across Canada and Alaska *Geophys. Res. Lett.* **33** L09703

Key C H and Benson N C 2006 *Landscape Assessment (LA)* (USDA Forest Service)

Kharuk V I, Ponomarev E I, Ivanova G A, Dvinskaya M L, Coogan S C P and Flannigan M D 2021 Wildfires in the Siberian taiga *Ambio* (available at: http://link.springer.com/10.1007/s13280-020-01490-x)

Kharuk V I, Ranson K J, Dvinskaya M L and Im S T 2011 Wildfires in northern Siberian larch dominated communities *Environ. Res. Lett.* **6** 045208

Kirillina K, Shvetsov E G, Protopopova V V, Thiesmeyer L and Yan W 2020 Consideration of anthropogenic factors in boreal forest fire regime changes during rapid socio-economic development: case study of forestry districts with increasing burnt area in the Sakha Republic, Russia *Environ. Res. Lett.* **15** 035009

Kolden C A, Lutz J A, Key C H, Kane J T and van Wagtendonk J W 2012 Mapped versus actual burned area within wildfire perimeters: characterizing the unburned *For. Ecol. Manage.* **286** 38–47

Krylov A, McCarty J L, Potapov P, Loboda T, Tyukavina A, Turubanova S and Hansen M C 2014 Remote sensing estimates of stand-replacement fires in Russia, 2002–2011 *Environ. Res. Lett.* **9** 105007

Loboda T V and Csiszar I A 2007 Reconstruction of fire spread within wildland fire events in Northern Eurasia from the MODIS active fire product *Glob. Planet. Change* **56** 258–73

Loranty M M, Lieberman-Cribbin W, Berner L T, Natali S M, Goetz S J, Alexander H D and Kholodov A L 2016 Spatial variation in vegetation productivity trends, fire disturbance, and soil carbon across arctic-boreal permafrost ecosystems *Environ. Res. Lett.* **11** 095008

Mack M C, Bret-Harte M S, Hollingsworth T N, Jandt R R, Schuur E A G, Shaver G R and Verbyla D L 2011 Carbon loss from an unprecedented Arctic tundra wildfire *Nature* **475** 489–92

Mack M C, Walker X J, Johnstone J F, Alexander H D, Melvin A M, Jean M and Miller S N 2021 Carbon loss from boreal forest wildfires offset by increased dominance of deciduous trees *Science* **372** 280–3

Masrur A, Petrov A N and DeGroote J 2018 Circumpolar spatio-temporal patterns and contributing climatic factors of wildfire activity in the Arctic tundra from 2001–2015 *Environ. Res. Lett.* **13** 014019

McLauchlan K K *et al* 2020 Fire as a fundamental ecological process: research advances and frontiers ed G Durigan *J. Ecol.* **108** 2047–69

MTBS 2016 Monitoring trends in burn severity assessment of fire information (Sioux Falls: U.S. Geological Survey and U.S. Forest Service (available at: www.mtbs.gov/direct-download)

Natali S M, Holdren J P, Rogers B M, Treharne R, Duffy P B, Pomerance R and MacDonald E 2021 Permafrost carbon feedbacks threaten global climate goals *Proc. Natl Acad. Sci. USA* **118** e2100163118

Olson D M *et al* 2001 Terrestrial ecoregions of the world: a new map of life on earth *BioScience* **51** 933
Pebesma E 2018 Simple features for R: standardized support for spatial vector data *R. J.* **10** 439–46
Ponomarev E, Kharuk V and Ranson K 2016 Wildfires dynamics in Siberian larch forests *Forests* **7** 125
R Core Team 2018 *R: A Language and Environment for Statistical Computing* (Vienna: R Foundation for Statistical Computing)
Rocha A V, Loranty M M, Higuera P E, Mack M C, Hu F S, Jones B M, Breen A L, Rastetter E B, Goetz S J and Shaver G R 2012 The footprint of Alaskan tundra fires during the past half-century: implications for surface properties and radiative forcing *Environ. Res. Lett.* **7** 044039
Roy D P, Boschetti L, Justice C O and Ju J 2008 The collection 5 MODIS burned area product—global evaluation by comparison with the MODIS active fire product *Remote Sens. Environ.* **112** 3690–707
Roy D P, Jin Y, Lewis P E and Justice C O 2005 Prototyping a global algorithm for systematic fire-affected area mapping using MODIS time series data *Remote Sens. Environ.* **97** 137–62
Roy D, Kovalskyy V, Zhang H, Vermote E, Yan L, Kumar S and Egorov A 2016 Characterization of Landsat-7 to Landsat-8 reflective wavelength and normalized difference vegetation index continuity *Remote Sens. Environ.* **185** 57–70
Shvidenko A Z, Shchepashchenko D G, Vaganov E A, Sukhinin A I, Maksyutov S S, McCallum I and Lakyda I P 2011 Impact of wildfire in Russia between 1998–2010 on ecosystems and the global carbon budget *Dokl. Earth Sci.* **441** 1678–82
Sizov O, Ezhova E, Tsymbarovich P, Soromotin A, Prihod'ko N, Petäjä T, Zilitinkevich S, Kulmala M, Bäck J and Köster K 2021 Fire and vegetation dynamics in north-west Siberia during the last 60 years based on high-resolution remote sensing *Biogeosci. Discuss.* **18** 207–28
Sofronov M A and Volokitina A V 2010 Wildfire ecology in continuous permafrost zone *Permafrost Ecosystems: Siberian Larch Forests* (Berlin: Springer) pp 59–82
Soja A J 2004 Estimating fire emissions and disparities in boreal Siberia (1998–2002) *J. Geophys. Res.* **109** D14S06
Soja A J, Shugart H H, Sukhinin A, Conard S and Stackhouse P W 2006 Satellite-derived mean fire return intervals as indicators of change in Siberia (1995–2002) *Mitig. Adapt. Strateg. Glob. Change* **11** 75–96
Soja A J, Tchebakova N M, French N H F, Flannigan M D, Shugart H H, Stocks B J, Sukhinin A I, Parfenova E I, Chapin F S and Stackhouse P W 2007 Climate-induced boreal forest change: predictions versus current observations *Glob. Planet. Change* **56** 274–96
Stephens S L *et al* 2014 Temperate and boreal forest mega-fires: characteristics and challenges *Front. Ecol. Environ.* **12** 115–22
Stephenson N 1998 Actual evapotranspiration and deficit: biologically meaningful correlates of vegetation distribution across spatial scales *J. Biogeogr.* **25** 855–70
Stocks B J *et al* 1998 Climate change and forest fire potential in Russian and Canadian boreal forests *Clim. Change* **38** 1–13
Stocks B J *et al* 2002 Large forest fires in Canada, 1959–1997 *J. Geophys. Res.* **108** 8149
Strauss J *et al* 2017 Deep Yedoma permafrost: a synthesis of depositional characteristics and carbon vulnerability *Earth Sci. Rev.* **172** 75–86
Strimas-Mackey M 2021 smoothr: smooth and tidy spatial features (available at: https://strimas.com/smoothr/index.html)
Talucci A C, Loranty M M and Alexander H D 2021 Fire perimeters for eastern Siberia taiga and tundra from 2001-2020 (https://doi.org/10.18739/A2N87311N)
Tedim F *et al* 2018 Defining extreme wildfire events: difficulties, challenges, and impacts *Fire* **1** 9
Teucher A, Russel K and Bloch M 2021 rmapshaper: client for "mapshaper" for "Geospatial" operations (available at: https://cran.r-project.org/web/packages/rmapshaper/index.html)
Turner M G, O'Neill R V, Gardner R H and Milne B T 1989 Effects of changing spatial scale on the analysis of landscape pattern *Landscape Ecol.* **3** 153–62
Walker L R, Wardle D A, Bardgett R D and Clarkson B D 2010 The use of chronosequences in studies of ecological succession and soil development: chronosequences, succession and soil development *J. Ecol.* **98** 725–36
Warren S G, Hahn C J, London J, Chervin R M and Jenne R L 1986 *Global Distribution of Total Cloud Cover and Cloud Type Amounts over Land* (Boulder, CO: National Center for Atmospheric Research)
Wickham H *et al* 2019 Welcome to the Tidyverse *JOSS* **4** 1686
Wooster M J 2004 Boreal forest fires burn less intensely in Russia than in North America *Geophys. Res. Lett.* **31** L20505
Wulder M A, White J C, Loveland T R, Woodcock C E, Belward A S, Cohen W B, Fosnight E A, Shaw J, Masek J G and Roy D P 2016 The global Landsat archive: status, consolidation, and direction *Remote Sens. Environ.* **185** 271–83
Young A M, Higuera P E, Duffy P A and Hu F S 2017 Climatic thresholds shape northern high-latitude fire regimes and imply vulnerability to future climate change *Ecography* **40** 606–17